Electron–nuclear double resonance on copper (II) tetraimidazole[a)]

Harlan L. Van Camp,[b)] Richard H. Sands,[c)] and James A. Fee[d)]

Biophysics Research Division, Institute of Science and Technology, The University of Michigan, Ann Arbor, Michigan 48109

(Received 15 January 1981; accepted 19 May 1981)

We have investigated the electron–nuclear double resonance (ENDOR) from frozen aqueous solutions of $^{65}Cu^{++}$(imidazole)$_4$, $^{65}Cu^{++}$ (imidazole-^{15}N)$_4$, and $^{65}Cu^{++}$(imidazole-D_n)$_4$, where $n = 1$, 2, 3, and 4 for selectively deuterated imidazole. We have observed ENDOR associated with the imidazole protons and the two imidazole nitrogens. The selective deuteration has allowed us to attempt identification of the weakly coupled protons responsible for the ENDOR spectrum, and a comparison of the overall line shape of that spectrum taken at two extreme points of the EPR spectrum suggests that some of the imidazole planes are tilted with respect to the plane of the complex. The ENDOR arising from the nitrogen nearest the copper is primarily isotropic with $A(g_\perp) = 41.6 \pm 1.5$ MHz and $A(g_\parallel) = 39.8 \pm 1.5$ MHz. The resonance shows little structure and seems consistent with a picture that requires some inequivalence among the various imidazoles. The remote nitrogen ENDOR reveals both hyperfine and quadrupole effects with approximately isotropic $A(^{14}N) = 1.79$ MHz, $Q_{z'z'} \simeq 0.360$ MHz, and $Q_{x'x'y'y'} \simeq 0.349$ MHz. These values are in agreement with the results of the nuclear modulation effect [J. Chem. Phys. **69**, 4921 (1978)]. The values for the quadrupole constants are thought to be accurate within 10% and are the same as are found in free imidazole. It is also demonstrated that, in this instance, ENDOR and the nuclear modulation effect are complementary in that they have each provided different parts of the same hyperfine spectrum.

INTRODUCTION

The imidazole moiety of histidine serves as a ligand to several metal ions associated with a broad class of conjugate proteins termed metalloproteins. These proteins perform such a diversity of chemical functions as to imply that the intimate structural details of the metal binding sites play an important role in effecting biological function. One tool for examination of detailed electronic structure of paramagnetic metal complexes is electron–nuclear double resonance (ENDOR). This spectroscopy has been successfully applied in a number of cases[1–3] to point out small details of structure within the metal binding sites of proteins. This derives from the ability of ENDOR to measure the interaction of the unpaired spin arising from the metal ion with magnetic nuclei in its immediate environment.

During the course of an ENDOR investigation of the Cu protein, superoxide dismutase [(H. Van Camp *et al.* (unpublished)], it was evident that the spectra obtained were not readily subject to simple interpretation. Therefore, as a precursive step, we decided to examine the ENDOR properties of the copper–tetraimidazole complex, whose major structural features closely approximate the Cu^{++} binding site of superoxide dismutase.[4] This model Cu-complex has provided us with the opportunity to control the isotopic composition of the ligand groups. For example, the normally present ^{14}N atoms can be replaced with ^{15}N, and the carbon bound protons can be selectively replaced with deuterons. In principle, it is possible to measure the degree of interaction between the unpaired electron of the Cu and several nearby atoms of the ligand group. In addition, it is possible to vary the solvent environment and examine its effect on the ENDOR spectra. After a discussion of methods used, we shall present and discuss the proton ENDOR, followed by the nearest neighbor and the remote nitrogen ENDOR. The latter has been investigated by Mims and Peisach[5] by the electron spin echo (ESE) technique. This study will be compared with that earlier one.

EXPERIMENTAL METHOD

The ENDOR spectrometer was constructed in this laboratory. It used homodyne detection with field modulation at either 100 KHz (Varian unit) or at 3 KHz (homemade unit). The microwave bridge operated at x-band and employed a reference arm enabling discrimination between absorption and dispersion. The details of the microwave ENDOR cavity are similar to those described elsewhere.[6]

The nuclear perturbing radio frequency (RF) was provided by a Hewlett-Packard 8601 generator and was amplified by an ENI 3100L 100 watt RF amplifier (though only about 10 watt was needed here). After phase detection and slight filtering, the signal was recorded on a Tracor Northern NS-570 signal averager. Electron paramagnetic resonance (EPR) was done in the absorption mode at a temperature of 77°K, but ENDOR was best obtained in the dispersion mode at 2°K. A typical Cu^{++} sample gave the best signal-to-noise ratio (S/N) at microwave powers of about 0.2 to 1 μW delivered to the cavity. The high field-modulation frequency and long relaxation times gave rise to rapid passage effects. The manipulation of those effects greatly influences the quality of the ENDOR spectra. For instance, the S/N increased with the RF sweep rate, but so also did dis-

[a)] Supported by an NIH Postdoctoral Service Award (H.V.C.) AM 05588, United States Public Health Service Research Grants, GM 12176 (R.H.S.) and GM 21519 (J.A.F.).

[b)] Present address: Bruker Instruments, Inc., Manning Park, Billerica, Mass. 01821.

[c)] Department of Physics.

[d)] Department of Biological Chemistry. Address inquiries to this author at the Biophysics Research Division, 2200 Bonisteel Blvd., Ann Arbor, Mich. 48109.

 0021-9606/81/172098-10$01.00

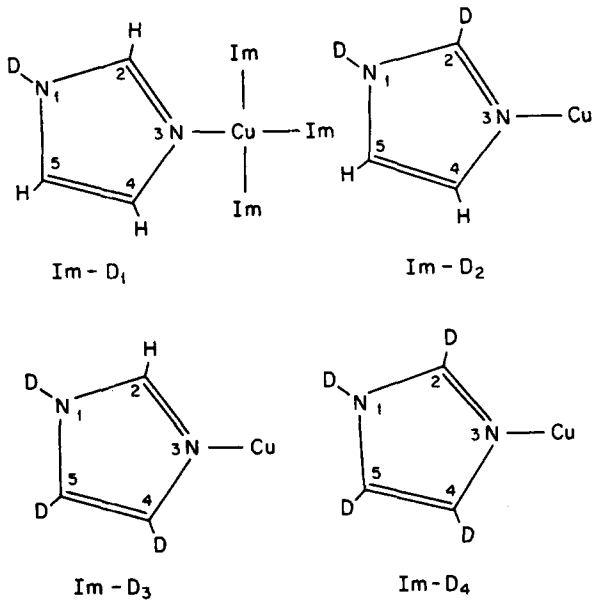

FIG. 1. Schematic representation of the four selectively deuterated imidazoles in $Cu^{++}(C_3H_4N_2)$. The notation, $Im-D_n$, refers to an imidazole having n deuteriums attached to either the carbons C_2, C_4, C_5, or the amine nitrogen. The nitrogen adjacent to the copper is referred to as the near-neighbor nitrogen in the text, and the nitrogen between C_2 and C_5 is referred to as the remote nitrogen.

tortion effects related to relaxation.[7] The latter introduced a skewness to the line shape and a shift in resonance position. Consequently, some compromise between S/N and distortion was usually reached, and in particular, line positions were deduced from the combination of forward and backward sweeps across the line. In addition to the above observation, it was found that the superposition of a small frequency modulation ($\Delta f \ll f$) on top of the radio frequency, f, increased the S/N (at the field modulation lock-in amplifier output) approximately linearly with the frequency deviation, Δf. This proved useful when looking for weak resonances, and was occasionally employed, provided the apparent ENDOR linewidth greatly exceeded Δf.

PREPARATIONS

Aqueous samples of $^{65}Cu^{++}(Im)_4$ were prepared in the following way. About 70 to 90 μmole of imidazole were mixed with 500 to 600 μl of glass distilled water. This solution was brought to one ml by the addition of glycerol, and was usually buffered at pH 8.0 with 0.5 M phosphate. One μmole of ^{65}Cu was then introduced with mixing and was immediately frozen in liquid nitrogen. Optical and EPR titrations showed that a large excess of imidazole was needed in order to insure saturation of the equatorial copper bonds. The need for relatively high concentrations of imidazole has been reported by other workers.[8,9]

It is known[10] that one obtains better resolution in the EPR spectrum by minimizing the dipolar broadening that ensues from species aggregation. To prevent aggregation one usually tries to obtain a glassy sample during the freezing process. Our ENDOR resolution was likewise dependent on such frozen dilution and was particularly sensitive to the pH, copper and glycerol concentrations. Although our ENDOR S/N was excellent at copper concentrations as high as 7 mM, we generally avoided concentrations greater than 2 mM because of the apparent formation of mixed species, which may also have signaled the onset of aggregation.

Preparation of ^{15}N enriched $^{65}Cu^{++}(Im)_4$ was similar to the above except for the initial separation of Cl^- from the acidic form of imidazole-^{15}N supplied by Stohler Isotope. The abundant magnetic Cl^- isotopes might have led to additional hyperfine splitting, further complicating the spectra.

The preparation of selectively deuterated imidazoles schematically represented in Fig. 1 made use of the pH–temperature profiles and procedures given by Vaughan *et al.*[11] $Im-D_1$ was made by drying imidazole in D_2O. But to make $Im-D_3$, one followed sequentially the procedures for $Im-D_4$, $Im-D_2$, and $Im-D_1$ with H_2O replacing D_2O in the middle step. Final products of the deuterations were freeze dried and recrystallized from warm benzene. Salt (NaCl) present in the deuteration process was removed by filtration over glasswool during the crystallization step. Verification that the selective deuteration had occurred was performed using a Varian T-60 NMR spectrometer. Final preparation of the $^{65}Cu^{++}(Im-D_n)_4$ samples was the same as that given above except for the use of 0.3 M KD_2PO_4 during the buffering step, and the use of glycerol-D_8. Completely deuterated glycerol was found to be absolutely necessary since the protons from even glycerol-D_3 produced an unwanted matrix ENDOR signal.

RESULTS AND DISCUSSION

Before recording ENDOR spectra one must examine the EPR spectrum in order to select a set of orientations for ENDOR. We display a trace taken at 77 °K in Fig. 2. The apparently axial spectrum clearly shows three of the four $^{65}Cu^{++}$ hyperfine peaks centered about $g_\parallel \simeq 2.255$. The fourth is hidden under the nitrogen superhyperfine structure (SHF) in the vicinity of 3200 G; the splitting of the latter is about 15 G. The lowest field ^{65}Cu hyperfine peak (near 2600 G) is resolved into nine smaller peaks, which for $I=1$ corresponds to four equivalent nitrogens. Their splitting is approximately 12.5 G. ENDOR measurements were most often performed at the extreme field limits of the EPR spectrum (indicated by the arrows in Fig. 2) because these positions were most likely to give double resonance results corresponding to predominately one orientation for the complex; for a square planar complex, this is especially true for the magnetic field in the orientation corresponding to $g_\parallel \simeq 2.255$.[12] At this g value, the magnetic field lies along the normal to the plane of the complex. On the other hand, the field direction corresponding to $g_\perp$ will lie within the plane of the complex.

We make a distinction here between the magnitudes of the fields corresponding to $g_\parallel$ (2.255), $g_\perp$ ($\simeq 2$), and $g_\parallel$-extreme (2.52), $g_\perp$-extreme (1.98). As shown in Fig. 2, the field corresponding to the $g_\parallel$-extreme (lowfield arrow) is set apart from the position of $g_\parallel$ because of

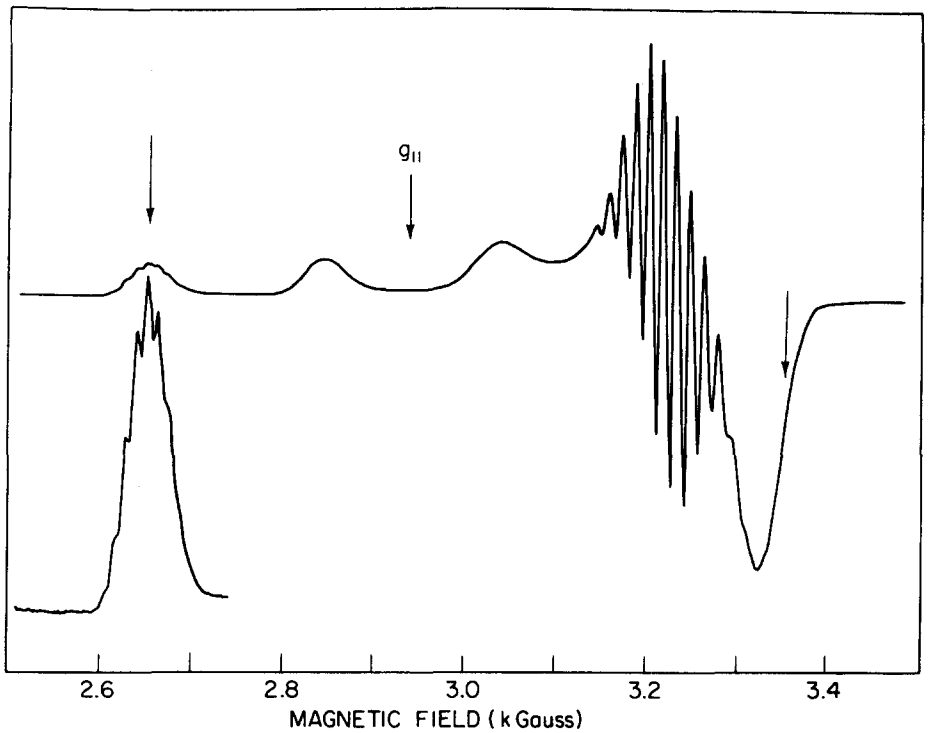

FIG. 2. Electron paramagnetic resonance spectrum of $^{65}Cu^{++}(Im)_4$. This sample was 1.6 mM in $^{65}Cu^{++}$ and contained about 50% glycerol. The arrows mark the approximate positions where most of the ENDOR was performed. An enlargement of the low field copper hyperfine peak shows evidence for four nearly equivalent nitrogens (nine superhyperfine peaks). Some instrumental conditions: temperature = 77°K, microwave power $\simeq$ 2 mW and frequency = 9.29 GHz, field modulation $\simeq 4G_{p-p}$ at 100 KHz, sweep = 1 KG in 5 min with time constant = 0.3 sec.

the presence of the copper hyperfine splitting ($\simeq$ 196 G). The associated hyperfine field of the copper is assumed to be parallel to the normal to the complex. If ENDOR were performed at the precise field value for $g_{\parallel}$, we would encounter complicating effects related to the anisotropy of the copper hyperfine structure. For the same reason, ENDOR performed at the $g_{\perp}$-extreme does not refer to an experiment done at the precise field value for $g_{\perp}$, but rather to ENDOR done at the high field extreme ($g = 1.98$). At this extreme, we are assuming that anisotropic effects associated with the EPR powder pattern will be lessened, and that the dominant contribution to ENDOR response will come from those molecules oriented so that the field is nearly within the plane of the complex. A precise value for $g_{\perp}$ was not measured in this work, but from Fig. 2 one expects it to occur within the superhyperfine structure near 3200 G (i.e., $g \simeq 2$).

Proton ENDOR

From proton ENDOR one wants to be able to identify the effects of specific protons and, if possible, to derive some information relevant to the particular molecular structure at hand. The latter is sometimes possible because of the significant dipolar contribution to the hyperfine coupling of weakly coupled protons.[13] We here present results which allow probable identification of the imidazole protons and suggest that the imidazole has been rotated in random fashion about the Cu–N axis.

Figures 3(a), 3(b), 3(c), and 3(d) show ENDOR from the four selectively deuterated complexes. The large peak appearing near 22 MHz in all of the traces is due to the nearest-neighbor nitrogen and will be discussed later. The series 3(a)–3(d), was taken at the $g_{\perp}$ extreme because this field position was the only one that brought out sharp structure in the proton region (9–17 MHz). Note that only the C_2–proton is present in Fig. 3(c). We therefore have positive identification of the maximum extent of its hyperfine effect at $g_{\perp}$. This is given by the frequency difference ($\simeq$ 5.2 MHz) between the two peaks centered about the free proton frequency, 13.2 MHz. Both the C_5 and C_4 protons are present in Fig. 3(b), and it would appear that the inner portion (with splitting = 1.7 MHz) is due to C_5–H and that the outer portion (with splitting = 5.28 MHz) is due to C_4–H. This conclusion seems attractive in view of Fig. 3(c), because of the steric symmetry between C_2–H and C_4–H. The identification must be considered as tentative, however, because in addition to the dipolar interaction between the unpaired electron and the proton there is also a contact interaction which may have a different value for the protons attached to C_2 and C_4. The observed hyperfine effect will be the sum of the contact and dipolar terms. The identification is tentative also because at $g_{\perp}$ the ENDOR response must be the result of the superposition of many orientations of the complex with respect to the static field $\mathbf{H}_0$. At best, such a powder pattern will involve those orientations for which $\mathbf{H}_0$ is in the Cu–N molecular plane. Thus it is more probable that the inner region of Fig. 3(b) contains contributions from both C_5 and C_4 protons. It is with the foregoing caution that we identify the contribution to the outer region of Fig. 3(b)

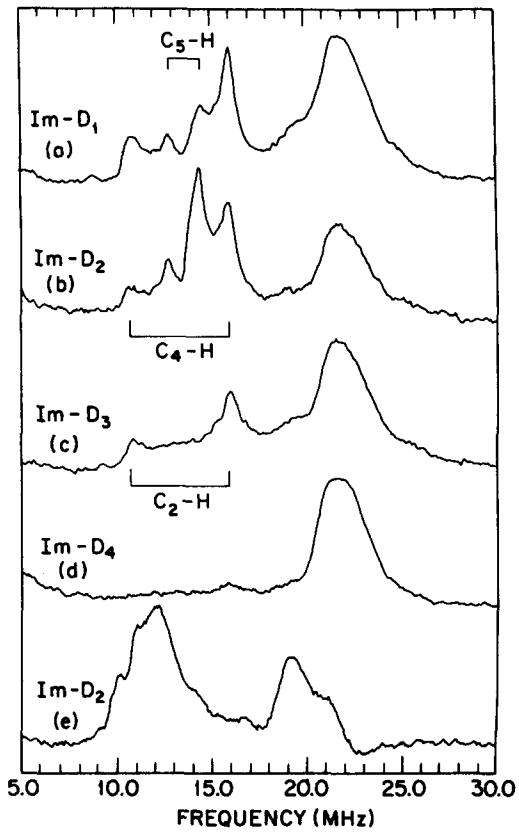

FIG. 3. ENDOR from selectively deuterated samples in completely deuterated solvent: (a) C_2, C_4, C_5 protonated, (b) C_4, C_5 protonated, (c) C_2 protonated, (d) completely deuterated, (e) trace taken at $g_{\parallel}$ extreme; note lack of resolution compared with (a), (b), and (c). Temperature is 1.8°K, sweep rate ≈ 0.25 MHz/sec, $g_{\perp}=1.98$ for (a, b, c, d), $g_{\parallel}=2.52$ for (e). Microwave power $\simeq 0.2$ w. Accumulation time for (b) was 40 min with a time constant of 0.5 sec.

as being due to the C_4–H proton.

Consider now the comparison between Figs. 3(a), 3(b), 3(c), and Fig. 3(e), which shows the best resolution found for Im–D_2 when H_0 is in the $g_{\parallel}$ direction. It is surprising that the sharpest features appear at the $g_{\perp}$ extreme and not at the $g_{\parallel}$ extreme. There are many examples in the literature of planar complexes where the reverse is true.[14,15] This is because, for axial symmetry, one usually expects the highest number of equivalent nuclei when H_0 is along $g_{\parallel}$; in ENDOR, increasing the number of equivalent nuclei reduces the number of resonances.

In order to qualitatively understand the proton results, we refer to a general expression for a proton ENDOR spectrum,

$$\nu_{\mathrm{ENDOR}}=\nu_p \pm \frac{1}{2}\left[A_c + D\sum\int \frac{\sigma_i}{|\mathbf{r}_p-\mathbf{r}_i|^3}(3\cos^2\theta_i - 1)d\tau\right], \tag{1}$$

where $\nu_p = g_N\beta_N H_0$ is the free proton frequency associated with the nuclear Zeeman effect, A_c is the contact hyperfine constant, σ_i is the unpaired electron spin density on the ith atom in the molecule, D is a constant, $\mathbf{r}_i$ and $\mathbf{r}_p$ are vector distances from an origin to the ith atom and the proton respectively, θ_i is the angle between H_0 and $(\mathbf{r}_p-\mathbf{r}_i)$, and $d\tau$ is the volume element in the electron distribution. The integral is needed when the electron orbital is sufficiently close to the proton that the former's extension in space cannot be neglected. This will be the case, for instance, for density on the adjacent carbon.[16] We must consider which terms in Eq. (1) may be distributed so as to produce a powder spectrum similar to Fig. 3(e).

Because of its effect upon the distribution of unpaired spin within the complex, a distribution of imidazole Cu^{++} bond lengths would presumably result in a spread of values for A_c, σ_i, or $|\mathbf{r}_p-\mathbf{r}_i|$, and these might lead to the observed broadening. However, we would expect a similar effect at $g_{\perp}$ but this is not observed. Crystallographic work on several crystalline compounds of Cu^{++}–imidazoles and/or imidazolates[17–20] have shown that the plane of the imidazole may be rotated about the Cu–N axis. The exact rotation angle appears to be determined by steric effects and hydrogen bonding between imidazole–H and the electronegative atoms present in nearby axial ligands. In our noncrystalline case, we envision that random hydrogen bonds between the imidazole and solvent are set up that then stabilize the tilted plane of the imidazole ring at some angle with respect to the Cu–N plane. This distribution of windmill-like molecules would present a spread in the angle θ_i even at the $g_{\parallel}$ extremum. This spread would not be so critical at $g_{\perp}$ since within the plane of the complex there are directions of the magnetic field for which θ_i will be constant (i.e., along a Cu–N direction).

Preliminary calculations, based upon the dipolar part of Eq. (1) together with reasonable estimates of the σ_i[21] were performed for the $g_{\parallel}$ case. A spread in the θ_i was generated by allowing all rotation angles of the plane of the imidazole to be equally probable (the actual spread in θ_i depends upon the particular proton and the site of the localized spin density). The broadening obtained from the calculation is about half that of the experimental trace. The calculations also yield sharp features at turning points that correspond to the imidazole plane being either normal to or coplanar with the plane of the complex. The presence of such turning points are unavoidable in powder spectra, and may be related to the hint of structure in Fig. 3(e).

Near-neighbor nitrogen ENDOR

The quality of the ENDOR response due to the near-neighbor nitrogens was similar at both ends of the EPR range. This response is represented by the somewhat indistinctive peaks near 20 MHz in Fig. 3. It is well known that a ^{14}N ($I=1$) nucleus coupled to an unpaired electron should present up to four peaks owing to the electron–nuclear hyperfine, nuclear Zeeman and nuclear quadrupole effects.[1,12] The first of these yields simply one, resonance centered at 1/2 the hyperfine constant ($A/2$). The nuclear Zeeman term splits this peak into two with a separation given by $2g_N\beta_N H_0$, where g_N and β_N are the nuclear magnetogyric ratio and nuclear magneton respectively. The third term will split each of these peaks into two more with a separation of

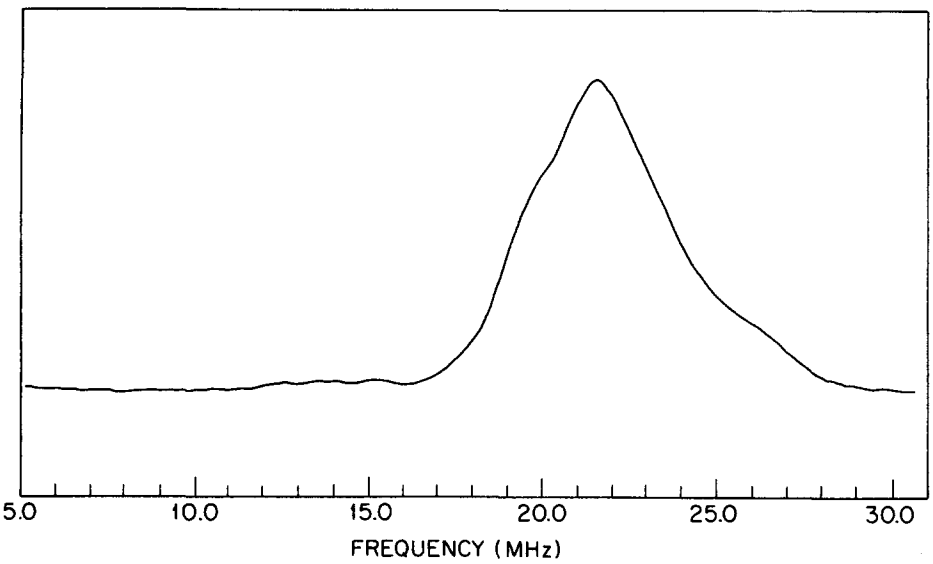

FIG. 4. ENDOR of completely deuterated sample taken at maximum of EPR dispersion signal, and corresponding to $g = 2.114$. At this g value the greatest S/N is found, but the spectrum is an unresolved powder pattern. Note the tail out to 26.5 MHz, which may be due to either nitrogen or ^{65}Cu. Temperature was 1.9 °K, sweep rate was 1.25 MHz/sec, accumulation time was about 5 min with time constant 0.2 sec. The shift in the spectrum due to the sweep rate is about 0.5 MHz toward a higher frequency.

twice the quadrupole energy along the effective field direction. Four peaks do not show up in Fig. 3, but Fig. 3(e) does show two unresolved features, which may be a nuclear Zeeman splitting. Here again we have an unexpectedly broad resonance. It may be relevant that broad line shapes have also been observed in the strongly coupled nitrogens present in several copper proteins: cytochrome-C oxidase,[3] stellacyanin,[2] and superoxide dismutase.

That this resonance is indeed due to the near nitrogen can be shown by the fact that the approximate hyperfine constants $A(g_\perp) = 41.6 \pm 1.5$ MHz and $A(g_\parallel = 39.8 \pm 1.5$ MHz agree well with the measured SHF splittings in the EPR spectrum. The lack of much anisotropy between these two extremes is consistent with dominant σ bonding that one expects here,[21,22] but we note that this anisotropy appears to be on the order of the linewidth. We further note that additional anisotropy is implied when ENDOR is performed at an intermediate g value (Fig. 4). The shoulder out near 26 MHz could be interpreted as due to the largest of three hyperfine components. One might also interpret it as being due to a copper hyperfine transition since the implied value of $A = 52$ MHz is not unrealistic for a square planar complex.[8,25] We have not made an exhaustive search for the copper ENDOR in this study, but we can mention that, because $I = 3/2$ for ^{65}Cu, one should expect up to six ENDOR transitions along with the characteristic nuclear Zeeman splitting of 7 MHz. We observed no such patterns during the course of this work. On the other hand, Roberts, Brown, Hoffman, and Peisach[26] have reported that the copper ENDOR in the protein stellacyanin is very broad (> 40 MHz) and has an opposite sense to that of the nitrogens and protons. We have observed a strong resonance which is approximately centered between the proton and near-nitrogen response and which also has an opposite sense. This signal is suppressed at the low microwave powers used for Fig. 3, but when the power is raised to 20–100 μW this spectral region (10–20 MHz) inverts losing all detail of the nitrogens and protons while adding little new detail. Although this is about where we might expect the copper hyperfine transitions to appear, we are somewhat reluctant to call this inverted signal "copper ENDOR" because a similar inversion behavior was observed at about the same frequency at the $g_\parallel$ extreme. And at this extreme the copper hyperfine constant is measurable by EPR (~ 196 G).

Some effort was put into discerning the nature of the poor resolution of the near-nitrogen ENDOR. Some possibilities include: (a) quadrupolar broadening, (b) concentration effects, (c) field modulation effects, (d) natural lifetime broadening, (e) completely noncrystalline ENDOR, and (f) slight inequivalence of imidazoles. We shall examine each of these in turn.

(a) Quadrupole broadening was ruled out by using ^{15}N–imidazole. The isotope, ^{15}N, has no quadrupole moment, but also brought no improvement in the resolution. It allowed us to place an upper limit of about 0.5 MHz on the effect of the quadrupole splitting of the ^{14}N. Although this is not an accurate measurement, we note that it implies a quadrupole coupling constant that is noticeably smaller than what has been observed for ^{14}N in many other compounds.[27] (b) Too large a concentration of copper, as mentioned earlier, can be detrimental to resolution. But variation of copper concentration over the range of 7 mM to 100 μM brought no improvement. (c) Broadening as a result of field modulation occurs as an artifact when sufficient anisotropy exists in the hyperfine parameters. When dealing with powder patterns, increments in field modulation amplitude correspond to increments in the angles that specify the orientation of the complex relative to the field direction. The field modulation corresponds to such a field increment, and

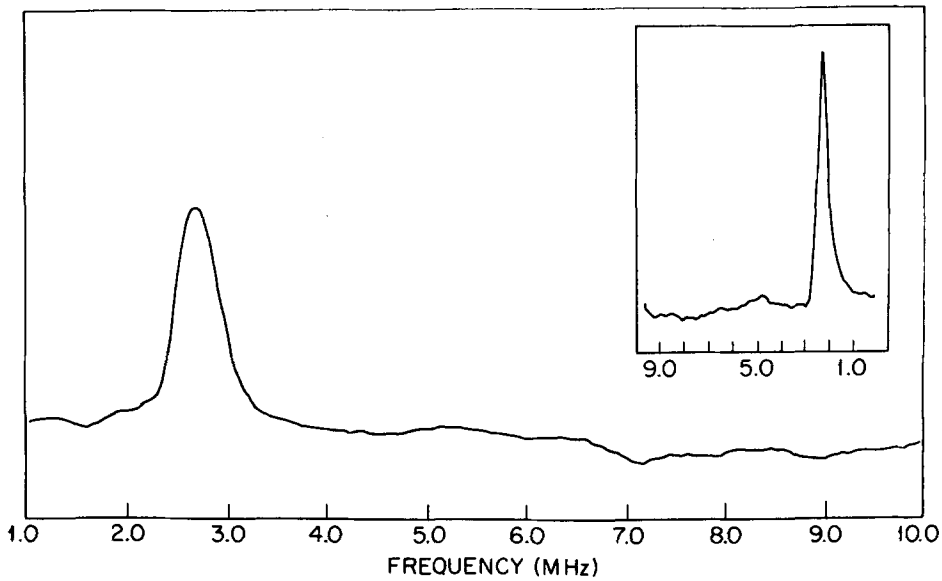

FIG. 5. Remote nitrogen ENDOR for ^{15}N enriched $^{65}Cu^{++}(Im)_4$. $g = 2.012$ $H_0 = 3032$ G, microwave power = 0.2 W and frequency = 8.537 GHz, temperature = 1.8 °K, field modulation = 1 G at 100 KHz, sweep rate was 0.18 MHz/sec, accumulation time was 53 min for increasing frequency, 26 min for decreasing frequency trace (inset). Average position of peak is at 2.56 MHz.

in our case the modulation was as large as 4 G which is very small compared with the overall width of the spectrum. So the increment in orientation incurred by 4 G modulation is likely to be small, especially at $g_{\parallel}$. (d) That the natural lifetime broadening should be so large is inconsistent with the comparatively narrow proton peaks seen at $g_{\perp}$. (e) Dalton[7] describes two extreme cases involving the ordering of the cross, T_x, and spin–lattice, T_1, relaxation times. When $T_x \gg T_1$ one can obtain single-crystalline ENDOR for some field values, but when $T_x \ll T_1$, one obtains the same powder spectrum for all field values. Because our proton spectrum shows anisotropy, it is likely that our case corresponds to $T_x \gg T_1$ and so crystal-like ENDOR spectra are possible. (f) Crystallographic studies of crystalline $Cu^{++}(Im)_4SO_4$ have determined two types of imidazole, one having a Cu–N distance of 2.000 Å, and the other with 2.021 Å.[18] Whether this particular inequivalence holds also for the glassy matrix is not known, and it may influence the contact term as well as the dipole term. Froncisz and Hyde[28] have shown that one can expect a distribution to arise in the value of $A_{\parallel}$ (Cu) when the sample solution is frozen. This along with a correlated spread in $g_{\parallel}$ is used to explain the linewidths of the copper hyperfine peaks in the $g_{\parallel}$ region. One may suppose that there is an associated spread in the ligand hyperfine constants as well. Finally we note that the spatial rotation of the imidazole plane to some arbitrary angle is a form of inequivalence already considered in the case of protons and should be considered here. Presumably the distribution of rotation angles would show up at least in the dipolar part of the hyperfine constant. We have noted at the beginning of this discussion that the expected anisotropy is at least on the order of the linewidth.

Remote nitrogen ENDOR

Mims and Peisach[5] have already detected the hyperfine interaction of the remote nitrogen in the spin echo nuclear modulation. From the modulation pattern they have constructed what would be an ideal ENDOR spectrum. Their interpretation depends on the coincidence that the hyperfine and nuclear Zeeman terms nearly cancel one another. Although our observations appear at first to differ from their construction, we shall show that the two observations are consistent and complementary.

As shown in Fig. 5, only one sharp line was observed in the 1 to 10 MHz region for $^{65}Cu^{++}(Im-^{15}N)$. When ENDOR is performed at the $g_{\perp}$ extreme, this line occurs at 2.56 MHz. The peak in Fig. 5 appears to be at 2.7 MHz, but this displacement is an artifact brought on by the sweep rate (0.18 MHz/sec). When the RF was swept with decreasing frequency at the same rate, the line shape was asymmetric in that it rose more abruptly than it descended (see inset of Fig. 5). When the frequency was swept in an increasing manner, this line appeared more nearly symmetric. When ENDOR was performed at $g_{\parallel}$, the ^{15}N peak shifted downfield to about 2.18 MHz. Such a shift is expected if the peak's position is in part determined by the nuclear Zeeman energy, which is proportional to the field. The sign of the shift suggests that a partner to this line exists at a much lower frequency.

Since ^{15}N has a nuclear spin of $I = 1/2$, there will be no quadrupole effects, and so we only have to deal with the Hamiltonian for the nuclear spin interacting with the external field $\mathbf{H}_0$, and the electronic spin S through a hyperfine constant A, i.e.,

$$\mathcal{H} = g_N \beta_N \mathbf{H}_0 \cdot \mathbf{I} + A\,\mathbf{S} \cdot \mathbf{I} .$$

We have taken the hyperfine constant to be isotropic (that is, negligible dipolar interaction). The Hamiltonian leads to ENDOR transitions given by

$$\nu = g_N \beta_N H_0 \pm \tfrac{1}{2} A = \nu_0 \pm \tfrac{1}{2} A . \quad (2)$$

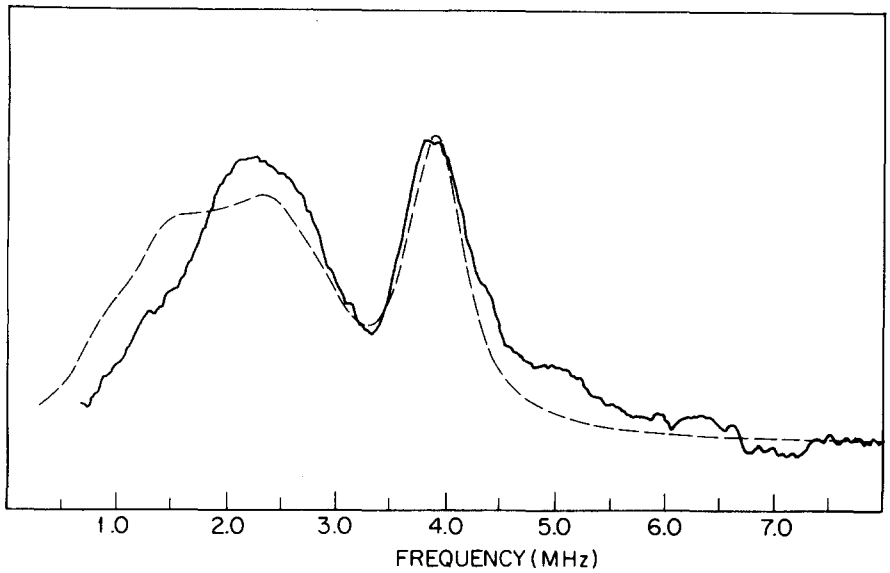

FIG. 6. Remote nitrogen ENDOR for $^{65}Cu(Im)_4$ with ^{14}N. Settings were similar to those in trace 5 except that the accumulation time (2 h) was longer because of the weaker peak intensity. The experimental trace (showing noise) has been shifted back 0.32 MHz in order to compare it with the computed trace (dashed line), which has been calculated for average line positions. The computed trace accumulated transitions for H_0 in the plane of the complex and for a rigid imidazole held normal to this plane.

We find that at $g_\perp$ a value of $A = 2.49$ MHz is consistent with the peak at 2.56 MHz provided that a second transition occurs at 0.065 MHz. A cursory check in this region showed no peak. This is not unexpected, however, because the perturbing RF magnetic field will be modified by a factor proportional to[23,24]

$$\epsilon = \left(1 + \frac{M_s A}{\nu_0}\right), \tag{3}$$

where $M_s = \pm 1/2$ is the electronic magnetic quantum number. The transition intensities resulting from this enhancement effect will be proportional to ϵ^2. Using the derived value for the hyperfine constant together with the known value for ν_0 (for ^{15}N, $\nu_0 = 1.31$ MHz when $H_0 = 3032$ G), one finds that in this instance, the low frequency peak should be more than three orders of magnitude less intense than the observed high frequency peak. From the same isotropic Hamiltonian, we find that $A = 2.26$ MHz when the ENDOR is performed at the $g_\parallel$ extreme of the EPR line. This anisotropy amounts to about 1/2 the linewidth. Our value of $A(g_\perp) = 2.49$ MHz agrees with the value of 2.5 MHz obtained by Mims and Peisach[5] at a similar field position.

Remote ^{14}N ENDOR

The more complicated situation involving ^{14}N is shown by the solid line spectrum in Fig. 6. Taken at the $g_\perp$ extreme, this should be compared with Fig. 10 of Ref. 5, which is a simulated ideal powder ENDOR pattern. Although that simulation is consistent with the results of the nuclear modulation effect, there are some noticeable differences between it and Fig. 6 of this paper. Instead of three sharp peaks at 0.7, 1.4, and 4 MHz plus a broad peak centered at 2 MHz, we observe one fairly sharp peak near 3.86 MHz and a broad one centered near 2.21 MHz. The latter could not be seen using the nuclear modulation effect, which depends upon the identification of periodicities in the electron spin echo decay envelope for the determination of transition frequencies, and it is the sharper well-defined transitions that give rise to the most persistent periodic modulation patterns. As in the ^{15}N case, Mims and Peisach[5] relied on the approximate cancellation of the hyperfine and nuclear Zeeman interactions to help them understand their particular result. The cancellation will occur in either the $M_s = +1/2$ or the $M_s = -1/2$ manifold (which one depends on the sign of the hyperfine constant), but because ^{14}N has a quadrupole moment, it remains possible for the cancelled manifold to have an energy level scheme characteristic of just the quadrupole interaction. Transitions within this manifold will approximate pure quadrupolar transitions, and were in fact identified with the sharp transitions at 0.7 and 1.4 MHz. Transitions within the uncancelled manifold were associated with the 4 MHz transition and the weak, broad resonance at 2 MHz. Although the 2 MHz band was not clearly evident in the transforms (5), it could nevertheless be predicted from a knowledge of the hyperfine constant (see below) and the quadrupole constants that were consistent with their observed spectrum.

For the computer simulation of their idealized ENDOR powder pattern, Mims and Peisach[5] used a spherical model whereby the electronic g value was taken to be isotropic, and the orientation of the electron–nuclear direction with respect to that of the static field was assumed to be random for the complexes in the glassy matrix. Thus, in accumulating contributions to the spectral simulation the static field, H_0, was allowed to vary over the sphere.

The only transition frequencies that were sensitive to this variation were the ones that gave rise to the 2 MHz band. Thus, broadening arose from the anisotropy in the quadrupole interaction.

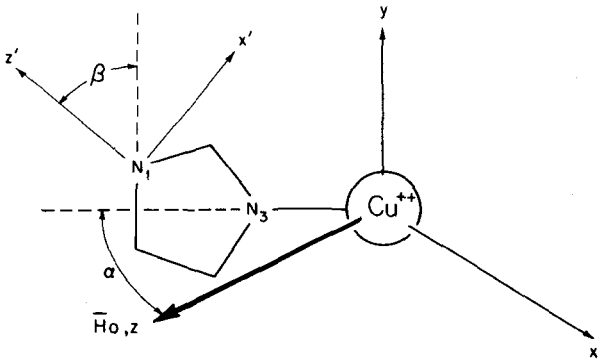

FIG. 7. Geometrical relationship of the imidazole and copper corresponding to the simulation shown in Fig. 6. The plane of the complex contains the z axis, $\mathbf{H}_0$, and the line passing through Cu–N. The direction of $g_{\parallel}$ or the y axis is normal to this plane. The plane of the imidazole is held normal to the plane of the complex so that the y' axis is directed into the page. The atomic coordinates for $Cu^{++}(Im)_4$ were taken from Fransson and Lundberg.[18]

In order to compare our two experimental results, we have synthesized an ENDOR spectrum starting with the interpretation of Mims. For the Cu^{++} $S=1/2$ interacting with the remote ^{14}N, we use the nuclear Hamiltonian,

$$\mathcal{H}=g_N\beta_N\mathbf{H}_0\cdot\mathbf{I}+A\mathbf{S}\cdot\mathbf{I}$$
$$+Q_{z'z'}[3I_{z'}^2-I(I+1)]+Q_{x'x'y'y'}(I_{x'}^2-I_{y'}^2)\ . \qquad (4)$$

We have again taken the hyperfine constant to be isotropic, and we have included quadrupolar terms. The principal axes of the latter terms, (x',y',z'), are defined as being different from those used to specify the quantization of the electron spin, e.g., (x,y,z), which in turn was specified within the high field approximation. The quadrupole principal axis system used here is shown in Fig. 7 and was taken from that determined by Ashby *et al.*[29] from the pure nuclear quadrupole resonance (NQR) of coordinated imidazole. The quadrupole interaction, expressed in this system, was then transformed to the reference frame determined by the resultant of the external and hyperfine fields, i.e., the effective field at the nucleus. Since we have taken the hyperfine interaction to be isotropic, the effective field will be colinear with the external field provided $\mathbf{H}_0$ is along a principal direction of the g tensor. In Fig. 7 we give the spatial relation between these two right-handed coordinate systems. When the quadrupole Hamiltonian $\mathcal{H}_Q$ is expressed in the (x,y,z) coordinate system, it becomes,

$$\mathcal{H}_Q=3Q_{z'z'}[\sin^2\beta(I_x^2\sin^2\alpha+I_z^2\cos^2\alpha)+I_y^2\cos^2\beta-\{I_x,I_z\}\sin^2\beta\cos\alpha\sin\alpha+(\{I_y,I_z\}\cos\alpha-\{I_x,I_y\}\sin\alpha)\sin\beta\cos\beta-2/3]$$
$$+Q_{x'x'y'y'}[I_x^2\sin^2\alpha\cos^2\beta-\cos^2\alpha)+I_y^2\sin^2\beta+I_z^2(\cos^2\alpha\cos^2\beta-\sin^2\alpha)$$
$$-\{I_x,I_z\}(\cos^2\beta+1)\cos\alpha\sin\alpha+(\{I_x,I_y\}\sin\alpha-\{I_y,I_z\}\cos\alpha)\cos\beta\sin\beta] \qquad (5)$$

where α is the angle swept out by $\mathbf{H}_0$ in the plane of the complex, β is the angle between the principal axis of the quadrupole interaction z' and the y axis, and $\{I_i,I_j\}=(I_iI_j+I_jI_i)$. We have made the natural choice of restricting the orientation of $\mathbf{H}_0$ to the plane of the complex because it is appropriate for ENDOR that has been done at the $g_{\perp}$ extreme of an axial EPR spectrum. The orientation of $\mathbf{H}_0$ was varied incrementally, and at each interval, the transition energies that proceed from Eqs. (4) and (5) were calculated for $M_s=\pm1/2$ by direct diagonalization of the 3×3 ($I=1$) secular matrix. Because the quadrupole and hyperfine terms are of comparable value, mixing of the hyperfine levels occurs that allows both $\Delta m_I=1$ and 2 transitions, but the influence of such mixing on the intrinsic intensity was not explicitly included here. Instead each transition was given a unit intensity, which was modified only by the magnitude of the de-enhancement effect given by Eq. (3). A histogram in frequency space was built up with a resolution of 0.032 MHz (i.e., 250 points per 8 MHz), and this was convoluted with a lineshape and normalized to the experimental spectrum. The initial calculations were performed using the computing facilities of the University of Michigan, and later calculations used a Bruker Aspect-2000 minicomputer.

A simulation corresponding to the geometry of Fig. 7 is shown by the dashed line in Fig. 6. Parameters were $A=1.79$ MHz, $g_N\beta_NH_0=0.95$ MHz ($H_0=3081$), $Q_{z'z'}=0.360$, and $Q_{x'x'y'y'}=0.349$ MHz. This value of A can be found by dividing the value of $A(^{15}N)$ by the ratio of the magnetic moments, i.e., 1.4. The values for $Q_{z'z'}$ and $Q_{x'x'y'y'}$ are derived from the NQR frequencies for protonated imidazole given by Hunt, *et al.*[30] and are the same values referenced by Mims. For this simulation, $\mathbf{H}_0$ was varied in the increments of 1°, and the plane of the imidazole was kept perpendicular to the plane of the complex so that the angle between $Q_{z'z'}$ and $g_{\parallel}$, i.e., β, was 50°. The line shape prior to convolution was taken to be Lorentzian, and we note that the use of a skewed line shape similar to that given by Dalton and Kwiram,[7] and which we have also observed would be expected to increase the intensity on the high frequency side of each resonance. The linewidth used was 0.6 MHz, and is only slightly greater than that of the ^{15}N peak in Fig. 4. The two sharp resonances at 0.7 MHz and 1.4 MHz in Fig. 10 of Ref. 5 are also present in our case, but they are reduced (as already mentioned) by the de-enhancement effect to far below the noise level. According to the zero linewidth calculation, the broad resonance at 2.2 MHz contains the powder pattern of the two allowed transitions that are the enhanced counterparts of the two missing peaks. In agreement with Mims and Peisach,[5] we find that the shape of the broad peak is most sensitive to the relative orientation of the imidazole and the field, $\mathbf{H}_0$, but we find that it appears to be

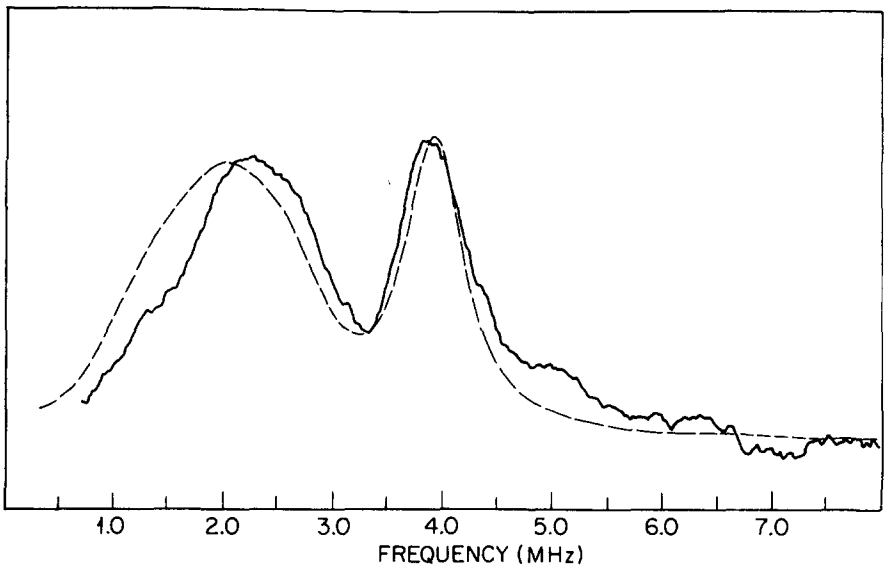

FIG. 8. Experimental trace (solid line) is compared to simulation (dashed line). Here the plane of the imidazole has been allowed to assume many orientations with respect to rotation about the Cu–N_3 axis. Increments of H_0 in the complex plane and increments of the imidazole rotation angle were each 2°. All anisotropic effects in Figs. 6 and 8 are quadrupolar.

biased onto the high side of 2 MHz both in experiment and in simulation. The peak near 4 MHz is a $\Delta m_I = 2$ transition, and shows little line shape dependence on the geometrical orientations of the complex relative to H_0.

Because consideration of the proton ENDOR spectra led us to believe that the plane of the imidazole could be tilted relative to the Cu–N plane, we calculated what effect this would have on the remote ^{14}N ENDOR simulation. For a given orientation of the imidazole plane, the external field was allowed to vary in 2° increments within the plane of the complex. This contribution to the histogram of transitions was then summed over imidazole orientations in 2° increments of the angle between the planes. The result is shown by the dashed line in Fig. 8. We note that it is symmetric about 2 MHz, but it too might be brought closer to experiment by use of the skewed line shape. Because details of the intrinsic ENDOR intensity were not attempted in this treatment, one cannot be too concerned with small differences in the local intensity between experimental and simulated traces. We can mention, however, that a feature such as the shoulder at 5 MHz was not duplicated for any of these imidazole orientations. In order to obtain a contribution there one would have to include an imidazole with significantly different parameter values. For example, a change of A from 1.79 to 3.0 MHz will shift the high frequency peak up to 5 MHz. Of the two simulations presented here, the fixed orientation seems slightly better insofar as peak position is concerned, but the random orientation simulation seems better with respect to line shape.

SUMMARY AND CONCLUDING REMARKS

We have investigated the ENDOR of $Cu^{++}(imidazole)_4$ as a precursive step leading to the understanding of the ENDOR in imidazole ligated copper proteins. We have discovered that three spectral regions of interest exist: proton, near-neighbor nitrogen, and remote nitrogen. The selective deuteration of imidazole has allowed the probable identification of the individual protons in the complex, and has raised the suggestion that some of the complexes may be inequivalent with respect to the relative orientations of the intramolecular imidazole planes. The ENDOR of the near nitrogens has shown little structure, but suggests an environment with little electric field gradient, a typically large isotropic hyperfine interaction, and an approximately axial anisotropic hyperfine interaction with the largest component being along an as yet undetermined direction. The remote nitrogen ENDOR spectra presented here appear to be different from that generated by the nuclear modulation experiments of Mims and Peisach, but we have shown that the two results are consistent with the same spin Hamiltonian, and are complementary in that what one method did not observe, the other did. In view of the fact that we seem to be observing delocalized spin density throughout the complex, it is remarkable that the values for the quadrupole constants correspond to free imidazole. Ashby *et al.*[29] have shown that the NQR frequencies depend on the coordination to Zn and Cd in a number of complexes. Shifts away from the free imidazole values for the quadrupole coupling constant of the amino nitrogen were reported to be as high as 24% [for $Zn(Im)_2Br_2$] and as low as 1% [for $Zn(Im)_2(C_6H_4O_2)$]. From the measurements reported here on $Cu(Im)_4$, we can say that the quadrupole constants of the remote nitrogen are probably not more than 10% different from the values for free imidazole. A change of 10% in $Q_{z'z'}$ and $Q_{x'x'y'y'}$ would correspond to a discernible shift of about 1% in the calculated position of the peak near 4 MHz. The less well defined band near 2 MHz would shift by about 4%.

ACKNOWLEDGMENTS

We wish to thank W. B. Mims, J. Peisach, C. P. Scholes, and W. R. Dunham for several helpful sugges-

tions. The former two kindly supplied us with the ^{15}N-imidazole. We also thank W. E. Downer and W. R. Dunham for help in the construction of the apparatus, D. O. Hershen for help in its operation, and K. Findling and A. Lees for help at certain stages of sample preparation.

[1]C. P. Scholes, R. A. Isaacson, and G. Feher, Biochim. Biophys. Acta 263, 448 (1972).
[2]G. H. Rist, J. S. Hyde, T. Vänngård, Proc. Natl. Acad. Sci. U. S. A. 67, 79 (1970).
[3]H. L. Van Camp, Y. H. Wei, C. P. Scholes, and T. E. King, Biochim. Biophys. Acta 537, 238 (1978).
[4]J. S. Richardson, K. A. Thomas, B. H. Rubin, and D. C. Richardson, Proc. Natl. Acad. Sci. U. S. A. 72, 1349 (1975).
[5]W. B. Mims and J. Peisach, J. Chem. Phys. 69, 4921 (1978).
[6]H. L. Van Camp, C. P. Scholes, and R. A. Isaacson, Rev. Sci. Instrum. 47, 516 (1976).
[7]L. R. Dalton and A. L. Kwiram, J. Chem. Phys. 57, 1132 (1972).
[8]R. E. Viola, C. R. Hartzell, and J. J. Villafranca, J. Inorg. Biochem. 10, 281 (1979).
[9]J. T. Edsall, G. Felsenfeld, D. S. Goodman, and F. R. N. Gurd, J. Am. Chem. Soc. 76, 3054 (1954).
[10]R. T. Ross, J. Chem. Phys. 42, 3919 (1965).
[11]J. D. Vaughan, Z. Mughrabi, and E. C. Wu, J. Org. Chem. 35, 1141 (1970).
[12]G. H. Rist and J. S. Hyde, J. Chem. Phys. 49, 2449 (1968).
[13]C. A. Hutchison Jr., Sixth International Symposium on Magnetic Resonance, Banff, Alberta, Canada (1977), p. 329.
[14]G. H. Rist and J. S. Hyde, J. Chem. Phys. 52, 4633 (1970).
[15]H. L. Van Camp, C. P. Scholes, C. F. Mulks, and W. S. Caughey, J. Am. Chem. Soc. 99, 8283 (1977).
[16]H. M. McConnell and J. Strathdee, J. Mol. Phys. 2, 129 (1959).
[17]G. Ivarsson, B. K. S. Lundberg, and N. Ingri, Acta Chem. Scand. 26, 3005 (1972).
[18]G. Fransson and B. K. S. Lundberg, Acta Chem. Scand. 26, 3969 (1972).
[19]G. Ivarsson, Acta Chem. Scand. 27, 3523 (1973).
[20]H. Freeman, Adv. Protein Chem. 22, 257 (1967).
[21]A. S. Brill, P. R. Kirkpatrick, C. P. Scholes, and J. H. Venable, Jr. in *Probes of Structure and Function of Macromolecules and Membranes*, edited by B. Chance (Academic, New York, 1971), Vol. 1.
[22]R. J. Sundberg and R. B. Martin, Chem. Rev. 74, 471 (1974).
[23]E. R. Davies and T. Rs. Reddy, Phys. Lett. A 31, 398 (1970).
[24]D. H. Whiffen, Mol. Phys. 10, 595 (1966).
[25]G. F. Bryce, J. Phys. Chem. 70, 3549 (1966).
[26]J. E. Roberts, T. G. Brown, B. M. Hoffman, and J. Peisach, J. Am. Chem. Soc. 102, 825 (1980).
[27]D. T. Edmonds, Phys. Rep. C 29, 233 (1977).
[28]W. Froncisz and J. S. Hyde, J. Chem. Phys. 73, 3123 (1980).
[29]C. I. H. Ashby, C. P. Cheng, and T. L. Brown, J. Am. Chem. Soc. 100, 6057 (1978).
[30]M. J. Hunt, A. L. Mackay, D. T. Edmonds, Chem. Phys. Lett. 34, 473 (1975).